

Numerical study of diffusion on a random-mixed-bond lattice

Devora Holder,^{*} Harvey Scher,[†] and Brian Berkowitz[‡]

Department of Environmental Sciences and Energy Research, Weizmann Institute of Science, Rehovot, Israel

(Received 5 November 2007; published 18 March 2008)

Diffusion on lattices with random mixed bonds in two and three dimensions is reconsidered using a random walk (RW) algorithm, which is equivalent to the master equation. In this numerical study the main focus is on the simple case of two different transition rates W_1, W_2 along bonds between sites. Although analysis of diffusion and transport on this type of disordered medium, especially for the case of one-bond pure percolation (i.e., $W_1=0$), comprises a sizable subliterature, we exhibit additional basic results for the two-bond case: When the probability p of W_2 replacing W_1 in a lattice of W_1 bonds is below the percolation threshold p_c , the mean square displacement $\langle r^2 \rangle$ is a nonlinear function of time t . A best fit to the $\ln\langle r^2 \rangle$ vs $\ln t$ plot is a straight line with the value of the slope varying with p, Δ, d , where $\Delta \equiv W_2/W_1$ and d is the dimension, i.e., $\langle r^2 \rangle \propto t^{1+\eta(p, \Delta, d)}$ with $\eta > 0$ for $\Delta > 1$. In other terms, all the diffusion ($\mathcal{D} \equiv \langle r^2 \rangle / 2t \propto t^\eta$) is anomalous superdiffusion for $p < p_c$ and $\Delta > 1$ for $d=2, 3$. Previous work in the literature for $d=2$ with a different RW algorithm established an effective diffusion constant \mathcal{D}_{eff} , which was shown to scale as $(p_c - p)^{1/2}$. However, the anomalous nature (time dependence) of $\mathcal{D}(t)$ becomes manifest with an expanded regime of t , increased range of Δ , and the use of our algorithm. The nature of the superdiffusion is related to the percolation cluster geometry and Lévy walks.

DOI: 10.1103/PhysRevE.77.031119

PACS number(s): 05.40.Fb, 05.60.-k, 02.50.-r

I. INTRODUCTION

There is an extensive and rich literature devoted to percolation [1] and random-bond systems. These systems have been the source of theoretical investigations of critical phenomena [1–3], models of disordered media [4], transport and diffusion (e.g., [5–7]), and a wide range of applications. One such application [8] was to determine the influence of fracture networks on the diffusion time of radioactive wastes through very low-permeability rock. The hydraulically disconnected fracture networks were modeled by anisotropic percolation clusters below the critical percolation value, p_c . A random walk (RW) algorithm was invoked to calculate the diffusion across a slab (thickness L) and determine the initial part of the first-passage-time distribution $F(L, t)$. The RW algorithm we used is equivalent to solving the standard transport equation, the master equation (ME); we denote it as the ME algorithm. Our motivation for the present study was the numerical determination of the full evolution of pure diffusion using this ME algorithm.

In the past, RW algorithms seem to have been derived in a somewhat arbitrary manner. De Gennes' "ant in a labyrinth" [9] has evolved into many subspecies of termites, all conceptually derived in attempts to better describe observed phenomena, but all lacking physical foundations. The use of the ME algorithm is shown here to lead to additional results in this classical problem of diffusion in the subcritical percolation domain.

Scaling aspects of the overall diffusion constant \mathcal{D}_{eff} in the subcritical percolation domain have been examined previously [5], with the finding that $\mathcal{D}_{\text{eff}} \propto (p_c - p)^{1/2}$, where p is

the probability of finding a bond with transition rate W_2 in the lattice. In this study we use the ME algorithm to investigate a prototype ($d=2, 3$)-dimensional random-bond system with transition rates $W=W_1, W_2$, concentrating on the region below or at the critical percolation (with $\Delta \equiv W_2/W_1$, and $p \leq p_c$, neglecting connected lattices). Our goal is to explore the evolution of pure diffusion in a mixed quasi-infinite domain. We demonstrate that an effective diffusion constant \mathcal{D}_{eff} is not defined over the values of p ($p \leq p_c$) and the range of t and lattice sizes that we explore. The basic result is that the mean square displacement $\langle r^2 \rangle$ is a nonlinear function of time t . A best fit to the $\ln\langle r^2 \rangle$ vs $\ln t$ plot is a straight line with the value of the slope varying with p, Δ, d , i.e., $\langle r^2 \rangle \propto t^{1+\eta(p, \Delta, d)}$ with $\eta > 0$ for $\Delta > 1$. Defining $\mathcal{D} \equiv \langle r^2 \rangle / 2t$, we have $\mathcal{D} \propto t^\eta$, i.e., anomalous superdiffusion. In many problems involving anomalous diffusion, the asymptotic behavior of the system is diffusive, but the time taken to reach this limiting behavior can be extraordinarily long (e.g., [10,11]). The present work clearly demonstrates this.

In the next section we derive the ME algorithm, in Sec. III we describe the numerical methods used, and in Sec. IV we exhibit the numerical results, the relation to solutions of the diffusion equation, and the difference between these results and those of [5], with a thorough discussion of the variance of $\langle r^2 \rangle$. To gain some insight into the phenomenon of superdiffusion in our case we relate, in Sec. V, the geometry of distributed percolation clusters to ideas based on Lévy walks [12], which also result in enhanced diffusion.

II. THE MASTER EQUATION FRAMEWORK FOR THE RANDOM WALK

We approach the problem of the kinetics of the particle motion in the random-mixed-bond system as a standard transport calculation. Our starting point for this multicompo-

^{*}devora.holder@weizmann.ac.il

[†]harvey.scher@weizmann.ac.il

[‡]brian.berkowitz@weizmann.ac.il

nent system is a master equation [13,14], which is simply a mass balance equation incorporating all the transition rates associated with each bond.

We cast the master equation into the form of a completely equivalent random-walk equation and derive $\psi_{s',s}(t)$, the probability per time that a transition occurs from $s \rightarrow s'$ (it is dependent on the location, i.e., each neighborhood is different in a specific representation):

$$\frac{\partial c(\mathbf{s},t)}{\partial t} = - \sum_{s'} w(s',\mathbf{s})c(\mathbf{s},t) + \sum_{s'} w(\mathbf{s},s')c(s',t), \quad (1)$$

where $c(\mathbf{s},t)$ is the normalized concentration or occupation probability and $w(\mathbf{s},s')$ is the transition rate from s' to \mathbf{s} ; the dimension of $\sum_{s'} w$ is reciprocal time. Following the development given in Appendix B in [15], and introducing

$$\mathcal{W}_s \equiv \sum_{s'} w(s',\mathbf{s}), \quad p(s',\mathbf{s}) \equiv w(s',\mathbf{s})/\mathcal{W}_s, \quad (2)$$

we obtain the result

$$\psi_{s',s}(t) = p(s',\mathbf{s})\psi_s(t), \quad (3)$$

$$\psi_s(t) = \mathcal{W}_s \exp(-\mathcal{W}_s t). \quad (4)$$

The time of the displacement in the ME algorithm is calculated using a random choice from the normalized distribution $\psi_s(t)$ in (4). The standard approach is to calculate the cumulative of the distribution, $\psi_s(t)$, set it equal to a random number $1-x$, $x \in (0,1]$, and solve for t . Hence, the transfer time is $t = -\ln(x)/\mathcal{W}_s$. It is important to note that in the ME algorithm the time is always controlled by the reciprocal of \mathcal{W}_s (2). This is in sharp contrast to the previous treatment of the ‘‘termite’’ and mixed diffusion case [5] (which we denote, hereafter, as the TM algorithm), in which the diffusion of a termite is considered with the same displacement probability $p(s',\mathbf{s})$ from the site \mathbf{s} to s' as in (2), but with a discrete time assignment of $1/w(s',\mathbf{s})$ for the chosen bond.

If the bonds originating from a site are all equal, the main difference between the ME and TM algorithms is the $\ln(x)$ factor and the coordination number of the lattice (this will be discussed in Sec. IV). However, at the boundary of a cluster the ME algorithm time calculation is significantly different from that of the TM algorithm, especially for $\Delta \gg 1$. As an example [in three dimensions (3D)], if there is one path available W_1 to exit from a (high-diffusion) cluster, the time calculation for the ME algorithm is inversely proportional to the sum of the transition rates on all possible paths, e.g., $-\ln(x)/(5W_2+W_1)$. The TM algorithm transition calculation for the exit would be $1/W_1$; the time differs by a factor of $(5\Delta+1)^{-1}$. The TM algorithm is intuitively appealing, but contradicts the master equation. The master equation takes into account the local neighborhood (i.e., all the bonds originating from a site) to calculate the probability per time to leave the site [$\psi_s(t)$]. While a particle hops off a node via one particular bond (with a particular transition rate) with a certain probability, the time for the particle to hop off the node will still depend on the local neighborhood. In the ME algorithm, it takes the same amount of time to hop off or back

into a cluster from one of its boundary sites. In the TM algorithm it can take a much greater time to hop off.

III. DIFFUSION SIMULATION

We have completed computer simulations of extended diffusion for many configurations in two and three dimensions. The system is constructed by bond percolation on an orthogonal lattice. For each configuration we cycle through every lattice bond and randomly place (using the NAG G05 random number generator algorithms) a W_2 bond with probability p and a W_1 bond (always set equal to 1) with probability $1-p$ (i.e., a cluster of W_2 bonds just spans the lattice at $p=p_c$). All of our results are for $p \leq p_c$. For numerically stable results, it proved necessary to use very large lattice sizes: 300^3 (in 3D) and 3000^2 (in 2D). Periodic boundary conditions were used, approximating the infinite boundary condition.

The general procedure for each RW was to parachute a particle to a random spot on the lattice and measure the distance squared, r^2 , using the initial position as the origin, as a function of time. Each complete set of RWs was generated with both the ME and the TM algorithms [5] according to the rules discussed in the previous section. We obtained $\langle r^2 \rangle$ for t up to 10 000; Δ was varied from 10 to 10 000. The bond density p was selected at intervals between 0 and 0.24 for 3D, $p_c=0.2488$, and 0.47 for 2D, $p_c=0.5$ (bond percolation [1]). To obtain $\langle r^2 \rangle$, we calculated r^2 for 5000 different walks on each lattice configuration, and then took the average of the mean value of r^2 over 20–40 different lattice configurations with the same value of p . This small number of lattice configurations produced a value of $\langle r^2 \rangle$ with very little error.

The variance in the mean values of r^2 over different simulations involving 5000 walks in a single lattice was small, and did not change drastically in time. However, the variance in the value of $\langle r^2 \rangle$ (an average over many lattice configurations) was significantly larger, and increased with time, with Δ , and with proximity to p_c . This problem was endemic to the small lattices (e.g., 150^3 for 3D and 300^2 for 2D) and was eliminated with the use of larger lattices (300^3 and 3000^2). This will be shown in Sec. IV.

In the one-component limit, $p=0$, the effective diffusion coefficient determined by $\langle r^2 \rangle$ equals that of the one-component medium, yielding a solution identical to that of the diffusion equation solved with \mathcal{D}_1 ($\mathcal{D}_1 = \frac{1}{2}na^2W_1$, n = lattice coordination number, a = lattice constant) on an infinite volume (setting $W_1=1$ and $a=1$ to define our units of length and time, i.e., t and lattice size are nondimensional).

IV. RESULTS

Our prototypical result is shown in Fig. 1. The mean $\langle r^2 \rangle$ at each value of p is computed from 5000 walkers in 20–40 configurations over a very long time interval. The variance in the average is shown at each value of $\langle r^2 \rangle$. To obtain such very small variances it was necessary to increase the size of the 3D lattice to 300^3 and the 2D lattice to 3000^2 . The form of $\langle r^2 \rangle$ is clearly not linear, and hence an effective diffusion

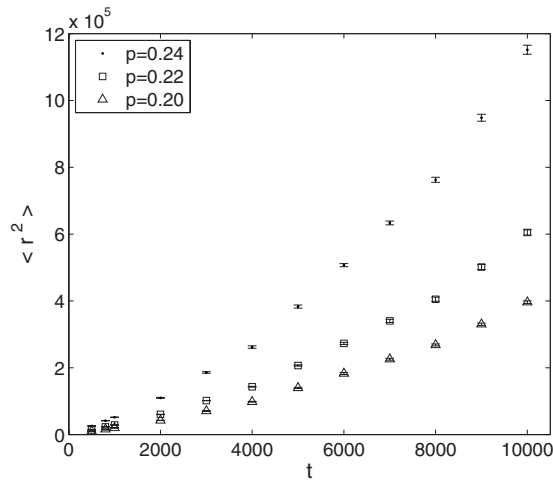


FIG. 1. $\langle r^2 \rangle$ vs t for $\Delta=10^4$, varying p for 3D lattices of size of 300^3 ; error bars represent the variance in $\langle r^2 \rangle$.

constant $D_{\text{eff}}=\langle r^2 \rangle/2t$ cannot be defined over the time range of the simulations. In general, for anomalous diffusion, the very long-time behavior asymptotes to a constant diffusion coefficient [16–18]. Even with our expanded time range, however, we do not see the evolution to this asymptotic behavior.

The nonlinearity of $\langle r^2 \rangle$ becomes more manifest with increasing Δ and t . The nonlinearity is subtle at early times but at later times becomes obvious. The data of Fig. 1 are shown in a log-log plot in Fig. 2. The best asymptotic fit to the data over this decade range is a linear plot; correlation coefficients of greater than 0.99 were found in all cases. It is expedient to use this power law summary of the data in the large-time limit, $\langle r^2 \rangle \propto t^{1+\eta}$. Hence, in this time range one has superdiffusion, i.e., $\eta > 0$. We show this result in Fig. 3 for various values of Δ in the range $\Delta \gg 1$, where the superdiffusive behavior increases with increasing Δ . In Figs. 4 and 5 the dependences (for 3D) of $1 + \eta$ on $p_c - p$ and Δ are exhibited, respectively. These dependencies will be discussed in the context of the percolation cluster structure in Sec. V.

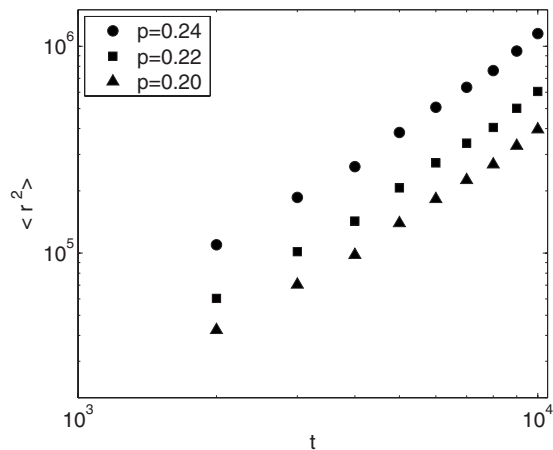


FIG. 2. Log-log plots of $\langle r^2 \rangle$ vs t (for $t > 10^3$, the asymptotic range) for $\Delta=10^4$, varying p for 3D lattices of size 300^3 .

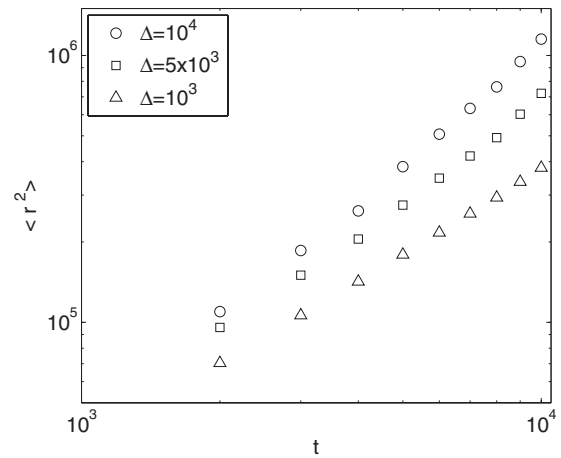


FIG. 3. Log-log plots of $\langle r^2 \rangle$ vs t for $p=0.24$, varying Δ for 3D lattices of size 300^3 .

The importance of the lattice size is seen clearly in Fig. 6, where the coefficient of variance of $\langle r^2 \rangle$ vs t is shown for lattices of sizes 100^3 and 300^3 . For the smaller lattices, the error bars grow with time and the shape of the curve of $\langle r^2 \rangle$ vs t for this lattice becomes unreliable. Figure 7 shows a comparison between the two algorithms discussed above. For a large value of Δ and a small $p_c - p$, the $\langle r^2 \rangle$ values determined with the two algorithms differ significantly in the degree of nonlinearity in t . The fitted exponents using the ME and TM algorithms are 1.46 and 1.13, respectively. Almost identical behavior was found for the 2D results.

The 2D results for the ME algorithm are shown in Fig. 8 for p ($=0.47$) close to p_c (2D) and varying Δ . These results are similar to Fig. 3 for the 3D case. This is also true for the comparison between the plots of $1 + \eta$ vs Δ in Figs. 9 and 5 for 2D and 3D, respectively.

Finally, the $\langle r^2 \rangle$ vs t plot in Fig. 10 is a validation of the use of the ME algorithm. We simulate diffusion in a uniform lattice of the same bonds ($\Delta=1$). The dependence of $\langle r^2 \rangle$ vs t is perfectly linear (i.e., $\langle r^2 \rangle=6t$ and $\langle r^2 \rangle=4t$). The coeffi-

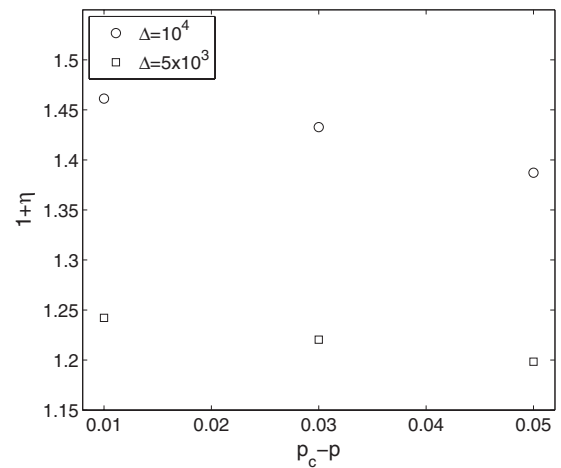


FIG. 4. Dependence of $1 + \eta$ on $p_c - p$ when Δ is varied for 3D results.

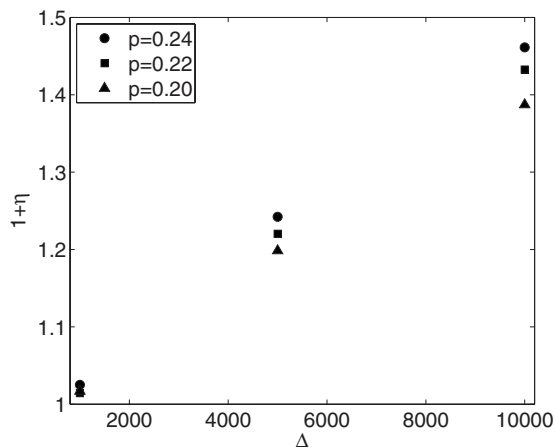


FIG. 5. Dependence of $1 + \eta$ on Δ when p is varied for 3D results.

icients 6 and 4 are the coordination numbers for 3D and 2D lattices, respectively. These coefficients do not appear when using the TM algorithm. In the units we chose, these relations are the same as the solution of the diffusion equation, since the second moment of the diffusion equation solution is $\langle x^2 \rangle = 2Dt$, and in the isotropic case ($\langle x^2 \rangle = \langle y^2 \rangle = \langle z^2 \rangle$), so $\langle r^2 \rangle = 2dDt$ (i.e., $\langle r^2 \rangle = 6Dt$ for the 3D results and $4Dt$ for the 2D results). In our units, $D = 1$.

V. CLUSTER GEOMETRY, LÉVY WALKS, AND SUPERDIFFUSION

The features of the geometry of percolation clusters for $p < p_c$ that we will use are its size distribution and ramified nature. As $p \rightarrow p_c$, a relatively small number of clusters grow large and at p_c one cluster spans the lattice. The probability of finding a cluster of size S for $p \leq p_c$ varies as $S^{-\tau}$ for S less than a cutoff size depending on p , where τ is referred to as

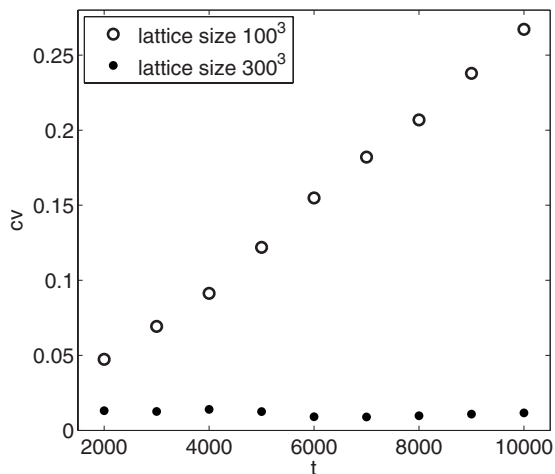


FIG. 6. Dependence of the coefficient of variance (CV) in $\langle r^2 \rangle$ (variance/mean) on t for $p = 0.24$, $\Delta = 10^4$ for 3D results. Data represent 80 realizations of 5000 particles on 100^3 lattices and 10 realizations of 5000 particles on 300^3 lattices.

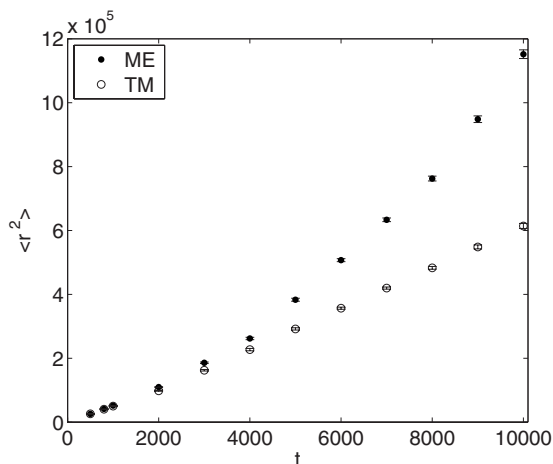


FIG. 7. $\langle r^2 \rangle$ vs t for $\Delta = 10^4$, $p = 0.24$ on 3D lattices for TM and ME algorithms. ME algorithm ran on 300^3 lattices, TM algorithm ran on 100^3 lattices; error bars represent the variance in $\langle r^2 \rangle$. Note: The TM algorithm results were multiplied by 6 (for 3D) and 4 (for 2D) to allow for comparison.

the cluster number. The radius of gyration R_S of a cluster varies with the size as $R_S^D \propto S$ [1], where D is referred to as the fractal dimension. The probability of encountering a cluster of length R_S varies as $R_S^{-\mu}$, where $\mu \equiv \tau D$. The ramified nature of these clusters plays a dynamic role in the effective diffusion on a single cluster.

The RW we simulate is one where there are nodes of standard diffusion (the W_1 bonds) and encounters with faster diffusion (the W_2 bonds) across lengths that are distributed as a power law ($R_S^{-\mu}$). This type of RW has similarities to a Lévy walk [12], in which there is a high probability for taking short steps, and, while long steps can occur, they are penalized with a longer time requirement. We relate these long steps to the displacement of a random walker over the length of a fast cluster, R_S , using our algorithm. We speculate that, as the overall position is nearly completely determined by the long, rare steps in the Lévy walk, the large, fast clus-

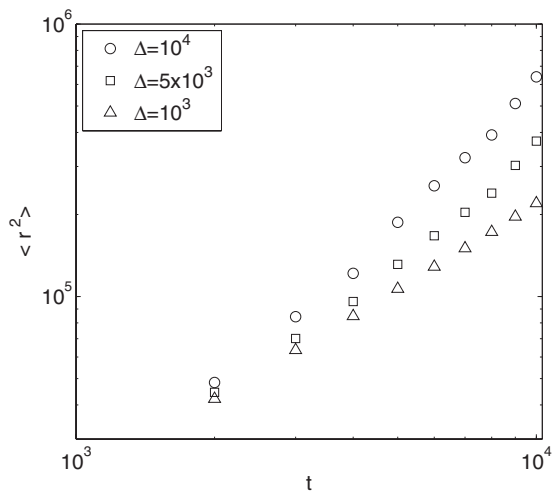


FIG. 8. $\langle r^2 \rangle$ vs t for $p = 0.47$, when Δ is varied for 2D lattices of size 3000^2 .

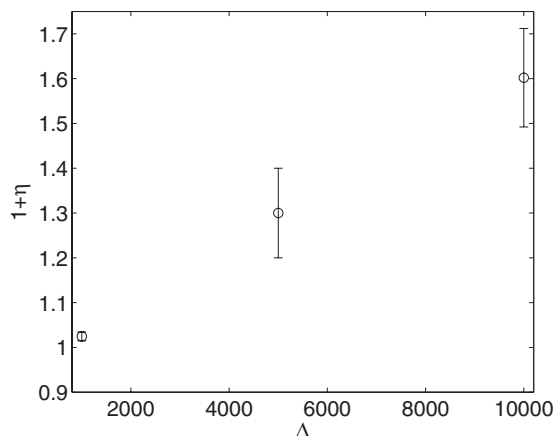


FIG. 9. Dependence of $1 + \eta$ on Δ for 2D results; $p=0.47$; error bars represent confidence levels of 95% for the slope of the fitted line to $\langle r^2 \rangle$ vs t data.

ters dominate the transport in our problem. In the asymptotic limit, the random walker encounters many of the larger finite clusters, and this averaging process can be expected to result in a well-defined diffusion coefficient.

Klafter *et al.* [12] use a continuous time random walk (CTRW) with a special space-time coupled joint distribution for the probability per time to have a displacement r in time t ,

$$\psi(\mathbf{r}, t) = Cr^{-\mu} \delta(r - t^\nu), \quad (5)$$

to generate a Lévy walk. The exponent μ controls the displacement probability, which we anticipate for our case is equal to τD . The exponent ν controls the type of transport during the displacement and the δ function couples r and t , imposing a time penalty that is coupled to the displacement length. We are interested in the value of γ in $\langle r^2 \rangle \propto t^\gamma$ produced with a CTRW using (5), and, in particular, the cases in which $\gamma > 1$. Klafter *et al.* [12] develop the exponent γ which depends on the interplay of the three arguments d , μ , and ν (two of which are combined into $\mu^* \equiv \mu - d + 1$).

The authors show in their Table I that, for the condition $\nu(\mu^* - 2) < 1$, $\gamma = 2 - \nu\mu^* + 2\nu$ when $\nu\mu^* > 2$, and $\gamma = 2\nu$ when $1 < \nu\mu^* < 2$. Hence, if μ^* is small enough (i.e., the probability for large displacements is large), there is a range of ν so that $\gamma > 1$. In our case we now show that $\nu\mu^* \sim 2$.

In the percolation geometry one has $\tau = 187/91$ and $D = 91/48$ for 2D and $\tau = 2.18$ and $D = 2.5$ for 3D, with the result that $\mu = 187/48 = 3.9$ and $\mu = 5.4$ for 2D and 3D, respectively [1]. For example, for 2D, if $\nu \leq 0.7$, one obtains $\gamma = 2\nu$. Hence, for the range of μ for the percolation geometry we have anomalous superdiffusion if $\nu \geq 0.5$.

In this picture, the superdiffusion through the percolation system depends on some enhancement of the diffusion in the individual cluster. Because these clusters are highly ramified, there is some admixture of diffusion across fast as well as slow bonds. On large clusters the encounters with boundary sites are frequent, so particles on clusters will tend to be accelerated through the cluster. As Δ increases the relative diffusion is enhanced. This is most likely due to the formation of preferential pathways through the cluster. Migration

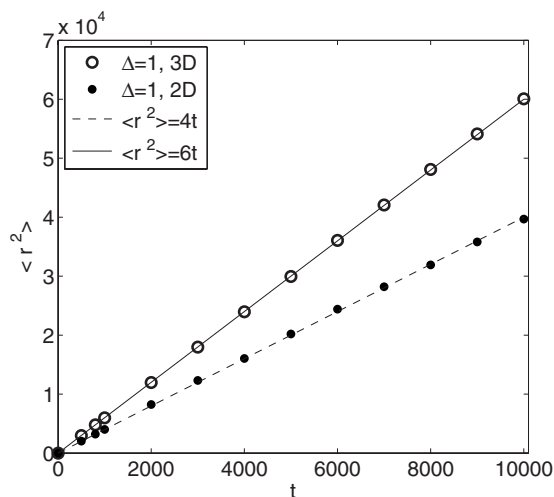


FIG. 10. $\langle r^2 \rangle$ vs t for 2D and 3D; $\Delta=1$ (uniform lattices of size 3000^2 for 2D and 300^3 for 3D). For 2D, data represent one realization; for 3D, data represent ten realizations. The lines are not fits, but rather overlaid plots of $\langle r^2 \rangle = 4t$ or $6t$ as indicated.

off the cluster is less likely as Δ increases. However, if a particle hops off a cluster, the time to make the transition using the TM algorithm is much greater than if using the ME algorithm [recall the factor $(5\Delta + 1)^{-1}$]. This may explain why, while the γ calculated using the TM algorithm (γ_{TM}) is superdiffusive, it is significantly smaller than γ_{ME} (recall Fig. 7).

Because μ^* is fixed, the maximum value of γ as a function of ν occurs for $\nu\mu^* = 2$, which is the upper limit for $\gamma = 2\nu$. The values of μ^* are 2.9 and 3.4 for 2D and 3D, respectively, so we observe that $\gamma = 2 - \nu\mu^* + 2\nu$ decreases as a function of ν , and therefore cannot produce a superdiffusive exponent. Note also that, because $\mu_{2D}^* < \mu_{3D}^*$, the values of ν can be larger for 2D (in keeping with $\nu\mu^* < 2$). Hence 2ν or γ ($\equiv 1 + \eta$) can be larger for 2D compared to 3D, which is in agreement with Fig. 9 compared to Fig. 5. According to [12], the maximum values of $1 + \eta$ are 1.4 for 2D and 1.2 for 3D. These values cover most of the range we calculated shown in Figs. 5 and 9. The higher values of $1 + \eta$ at very large Δ ($\sim 10^4$) are not accommodated in this analogy with the Lévy walk of (5) unless there is a small dynamic decrease in μ^* at the highest Δ . The comparison to the Lévy walk provides some insights into the mechanism of superdiffusion in this system of power law distribution of cluster lengths.

VI. SUMMARY

In this study, we explore transport on a subcritical mixed bond lattice using a RW algorithm, equivalent to the master equation, that generates superdiffusive behavior. We examine this system in 2D and 3D with an extended time regime and wide range of Δ . Using both the TM and the ME algorithms, it is concluded that, for long times, a constant \mathcal{D}_{eff} does not exist, and that $\mathcal{D} \propto t^\eta$ where η generated by the ME algorithm is greater than that of the TM algorithm. The time dependence of $\mathcal{D}(t)$ becomes apparent at long times, and increases

with Δ . An analogy to the Lévy walk (5) is proposed to provide some insights into this mechanism of superdiffusion. This surprising result is attributed to enhanced diffusion on large clusters with complex, ramified geometries.

ACKNOWLEDGMENTS

The financial support of the Guggenheim-Ascarelli Foundation is gratefully acknowledged.

-
- [1] D. Stauffer and A. Aharony, *Introduction to Percolation Theory*, 2nd ed. (Taylor and Francis, London, 1994).
- [2] J. P. Straley, *Phys. Rev. B* **15**, 5733 (1977).
- [3] M. E. Binney, J. J. Newman, N. J. Dowrick, and A. J. Fisher *The Theory of Critical Phenomena: An Introduction to the Renormalization Group* (Oxford University Press, London, 1992).
- [4] V. Ambegaokar, B. I. Halperin, and J. S. Langer, *Phys. Rev. B* **4**, 2612 (1971).
- [5] A. Bunde, A. Coniglio, D. C. Hong, and H. E. Stanley, *J. Phys. A* **18**, L137 (1985).
- [6] J. Adler, D. Aharony, and D. Stauffer, *J. Phys. A* **18**, L129 (1985).
- [7] A. Bunde and W. Dieterich, *J. Electroceram.* **5**, 81 (2000).
- [8] B. Berkowitz and H. Scher, *Geophys. Res. Lett.* **23**, 925 (1996).
- [9] P. G. De Gennes, *Recherche* **7**, 919 (1976).
- [10] S. Havlin, Z. V. Djordjevic, I. Majid, H. E. Stanley, and G. H. Weiss, *Phys. Rev. Lett.* **53**, 178 (1984).
- [11] E. Müller-Horsche, D. Haarer, and H. Scher, *Phys. Rev. B* **35**, 1273 (1987).
- [12] J. Klafter, A. Blumen, and M. F. Shlesinger, *Phys. Rev. A* **35**, 3081 (1987).
- [13] I. Oppenheim, K. E. Shuler, and G. H. Weiss, *Stochastic Processes in Chemical Physics: The Master Equation* (MIT Press, Cambridge, MA, 1977).
- [14] M. F. Shlesinger, *Random Processes*, Encyclopedia of Applied Physics Vol. 16 (VCH, New York, 1996).
- [15] B. Berkowitz, A. Cortis, M. Dentz, and H. Scher, *Rev. Geophys.* **44**, RG2003 (2006).
- [16] A. Cortis, Y. Chen, H. Scher, and B. Berkowitz, *Phys. Rev. E* **70**, 041108 (2004).
- [17] M. Dentz, A. Cortis, H. Scher, and B. Berkowitz, *Adv. Water Resour.* **27**, 155 (2004).
- [18] B. Bijeljic and M. J. Blunt, *Water Resour. Res.* **42**, W01202 (2006).